

Growth of ultrathin Fe films on Ge(100): Structure and magnetic properties

P. Ma

Department of Physics, University of Western Ontario, London, Ontario, Canada N6A 3K7

P. R. Norton

Department of Chemistry, University of Western Ontario, London, Ontario, Canada N6A 5B7

(Received 7 April 1997; revised manuscript received 25 June 1997)

The structure and magnetic properties of ultrathin Fe films grown on Ge(100) at room temperature have been studied by low-energy electron diffraction, Auger electron spectroscopy (AES), angle-resolved AES, and *in situ* magneto-optical Kerr effect (MOKE) measurements. Fe initially grows on Ge(100) in a disordered fashion, with local order commencing around 4 ML. The film grows with a bcc structure for thicknesses greater than 7 ML. Our data are consistent with 6% Ge intermixed in the films. Significant intermixing starts at about 160 °C, with rapid diffusion of Fe into the bulk occurring at temperatures higher than 400 °C. A single-loop to stepped-loop to single-loop sequence of ferromagnetic loops was observed by MOKE measurements. Hysteresis loop simulations were performed based on the coherent model, the results suggesting that strong in-plane uniaxial anisotropy exists in these films, especially for very thin films. The sequence of loops is due to the increase of the ratio between the cubic anisotropy and the uniaxial anisotropy as the film thickness increases. [S0163-1829(97)03239-6]

I. INTRODUCTION

The study of ultrathin ferromagnetic structures has been an active research field in recent years, due to the unique properties of such systems and the potential for new applications. The ability to grow magnetic structures directly on semiconducting surfaces has an additional attraction in that it might be possible to integrate magnetic devices and electronic circuits on a single chip.¹

The lattice constant of Ge is about twice of that of bcc Fe with only a 1.3% lattice mismatch. Together with the commercial availability of high-quality single crystal wafers, this makes Ge a very attractive substrate on which to grow bcc Fe films. However, there have not been many studies of ultrathin Fe films on Ge substrates, probably because of the concern that intermixing between the substrate and the deposits might create a thick magnetic dead layer. For example, it has been reported that the magnetic dead layer can be more than 100 Å thick for an Fe film grown on Ge at 150 °C.² A recent study of the growth of Fe on a S-passivated Ge(100) surface was successful in producing ferromagnetic Fe films with interesting magnetic properties.³ A much thinner dead layer (less than 10 Å) was observed for Fe grown on a S-passivated Ge(100) surface at 150 °C compared to the >100 Å magnetic dead layer of Fe grown on clean Ge(100) at the same temperature. This large difference of the thicknesses of the magnetically dead layers of Fe on clean Ge(100) and S-passivated Ge(100) indicates a need for further study of this system. We have therefore studied the growth of Fe on the Ge(100) surface at lower temperatures with emphasis on the composition and structure related to the magnetic properties.

In this paper, we present our study of the composition, structure, and magnetic properties of ultrathin Fe films grown on Ge(100) at room temperature. We use low-energy electron diffraction (LEED), Auger-electron spectroscopy

(AES), and angle-resolved AES (ARAES) to study the structure, composition, and growth of the films. The magneto-optic Kerr effect (MOKE) technique is used to characterize the magnetic properties of the thin films.

II. EXPERIMENT

All the preparation and structural characterizations of the thin films were performed in an ultrahigh vacuum (UHV) chamber (main chamber) with a base pressure of 1×10^{-10} torr. This chamber is equipped with rear view LEED optics and a VG CLAM electron energy analyzer for AES and ARAES. The LEED images can be recorded on video tape for spot intensity and width analysis by software of our own design. The main chamber is connected with another UHV chamber (MOKE chamber) for MOKE measurements. The sample can be transferred between these two chambers in vacuum, which allows us to perform *in situ* magnetic property measurements. The main chamber is also interfaced to a 2.5-MeV van de Graaff accelerator, for *in situ* Rutherford backscattering spectrometry (RBS), etc.

N-type Ge(100) wafers supplied by Superconix were used as substrates. After rinsing in methanol, the substrates were inserted into the vacuum chamber for cleaning. The surfaces were sputtered by 1.5-keV Ar⁺ ions at $0.5 \mu\text{A}/\text{cm}^2$ at 15° and -15° incidence angle for 10 min at each angle, and then annealed at 800 °C for 10 min. After this cleaning process, no contamination was detected with AES and a sharp (2×1) LEED pattern was observed. STM measurements (reported elsewhere⁴) on Ge(100) following the same cleaning procedure showed that the surface was well ordered and with large flat terraces. The Fe source is an *e*-beam evaporator and the flux was calibrated by RBS by measuring the amount of Fe deposited on a clean Si(100) surface under identical conditions. The Fe films were grown at room temperature without any further annealing. In this paper, 1 ML of Fe is

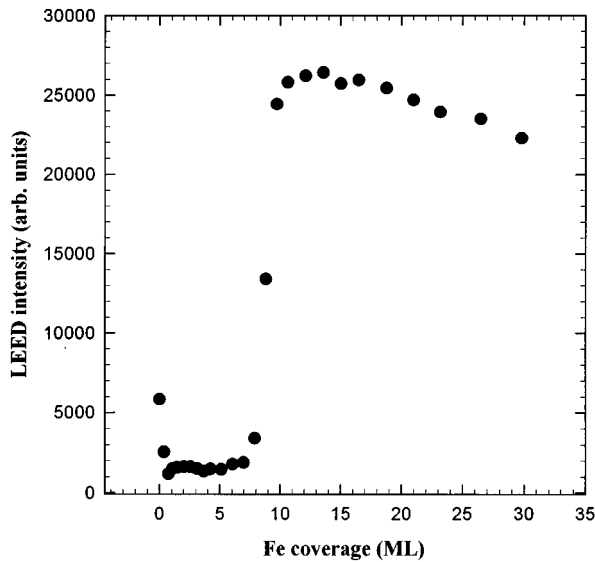


FIG. 1. LEED spot intensity ($[1,0]$ beams at 120 eV) as a function of Fe coverage.

defined as 1.22×10^{15} atoms/cm². All the *in situ* MOKE measurements were performed in the longitudinal configuration and the applied magnetic field was along the $\langle 010 \rangle$ direction of the sample. The *ex situ* MOKE measurements on gold capped Fe films were also made in the longitudinal configuration while the orientation of the applied field in the sample plane could be varied.

III. RESULTS AND DISCUSSION

A. Growth and structure of the Fe films

1. LEED study

After sputter cleaning and annealing at 800 °C, a sharp (2×1) LEED pattern was observed for the Ge(100) surface. Figure 1 shows the intensity of the diffraction beams of the coincident spots from Ge(100) and the Fe overlayer, as a function of Fe coverage. Deposition of Fe led to complete extinction of the Ge diffraction beams by coverages as low as 0.3 ML. No diffraction pattern from the substrate or overlayer Fe film was observed for coverages between about 0.3 and 7 ML. The diffraction pattern reappeared at about 8 ML. LEED pictures of the substrate and the Fe films of various thickness were taken at different primary energies, and the overlayer (Fe) first-order beams coincide with the Ge(100) second-order beams. This indicates that the lattice constant of the ordered Fe films is half of that of the substrate, i.e., the lattice constant of the overlayer is the same as that of bulk bcc Fe, and that the lattice orientation of the overlayer is registered with that of the substrate. This is consistent with the ARAES observations that will be presented in this section.

The recovery of the LEED pattern around 7 ML is a very steep function of Fe coverage, the major part of the effect being completed within about 3 ML. The spot intensity reaches its maximum value around 12 ML and then starts to decrease as more Fe is deposited.

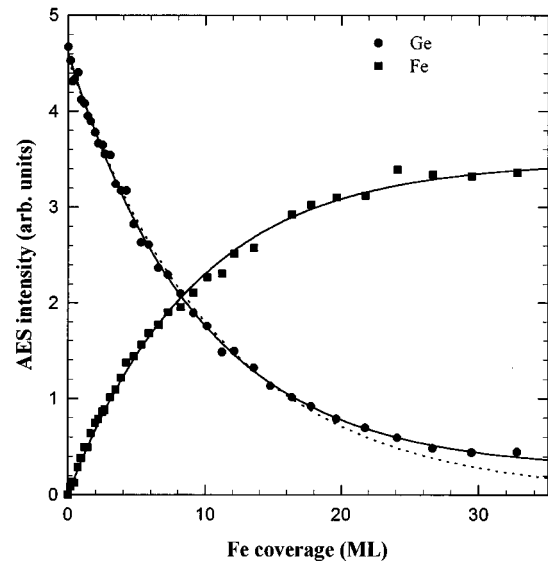


FIG. 2. Ge and Fe AES intensities as functions of Fe coverage. The lines are least-squares fits to the exponential functions (see text for details). In the Ge branch, the dotted line is the fit without an offset, while the solid line is the fit with an offset.

2. AES study

Figure 2 shows the AES intensity of the Ge *LMM* (1147 eV) and Fe *LMM* transitions at (706 eV) as a function of Fe coverage. The data points follow a smooth line and no apparent breaks were detected. The lines are the least-squares fittings to an exponential function (see below). The calculated attenuation lengths based on the fitting are 15.5 Å for the Ge 1147-eV Auger electrons and 13.2 Å for the Fe 706-eV Auger electrons, respectively. To extract information about the intermixing (if there is any) and the growth mode from the data, we have computed the attenuation for two simple models. One possibility is that there is a uniform intermixed region throughout the film, with a small percentage of incorporated Ge. Then, after depositing n ML Fe, the Ge AES intensity can be written as

$$B = B_t \exp(-nd_0/\lambda) + \sum_{n=1}^n \rho B_0 \exp[-(i-1)d_0/\lambda], \quad (1)$$

where B_t and B_0 are the AES intensities of bulk Ge and 1 ML Ge, respectively, ρ is the Ge atomic density in the film, d_0 is the monolayer thickness, and λ is the attenuation length of Ge Auger electrons in the film. The first term is the attenuated signal from the substrate and the second term is the signal from within the film. If we ignore the difference of the attenuation lengths of Ge Auger electrons in the film and in the bulk Ge, we have $B_t = B_0/[1 - \exp(-d_0/\lambda)]$. Therefore, the above equation can be simplified to

$$B = \rho B_t + B_t(1 - \rho) \exp(-nd_0/\lambda). \quad (2)$$

Here we see that for an intermixed film, in addition to the exponential dependence of the substrate signal on the film thickness, there is a constant background that is proportional to the atomic density of the substrate element in the intermixed film.

In the Ge data in Fig. 2, the solid line is the least-squares fit of the data to an exponential function with offset, while the dotted line is the fit to an exponential function without offset. We see that the fit that includes the offset is satisfactory, and that the other fit is not as good, especially at high Fe coverages. This suggests that intermixing does take place at some point. The estimated uniform Ge concentration is 6%.

A further possible model is one in which the constant background originates from a small amount of Ge segregated on top of the Fe film. In this model, after deposition of n ML Fe, the Ge AES intensity can be written as

$$B = B_t(1-x)\exp(-nd_0/\lambda) + B_tx \exp[-(1+n)d_0/\lambda] + xB_0, \quad (3)$$

where x is the monolayer coverage of the segregated Ge (assuming it is less than 1 ML and is the same for all Fe coverages), and other symbols are the same as in Eq. (1). The first two terms are the attenuated substrate signal and the third term is the signal from the segregated Ge. Using the relation between B_t and B_0 , Eq. (3) can be rearranged as

$$B = [B_t(1-x) + B_tx \exp(-d_0/\lambda)]\exp(-nd_0/\lambda) + xB_t[1 - \exp(-d_0/\lambda)]. \quad (4)$$

Again, we see the Ge AES intensity exhibits an exponential dependence on the Fe coverage with a constant background. Mathematically, Eqs. (4) and (2) are the same. Therefore, the best fits for Eqs. (2) and (4) to the data are the same and the calculated preexponential coefficients and the constant terms are also the same. The calculated Ge coverage is about 0.6 ML for the best fits.

To distinguish these two models, we grew a thick Fe layer (30 ML) on the Ge(100) substrate, and then monitored the AES intensities of Ge and Fe while Ar sputtering the film. For the segregation model, a significant drop ($\approx 36\%$ based on Fig. 2) of the ratio between Ge and Fe AES intensities is expected after the first one or two monolayers being removed. Figure 3 plots the AES ratio vs the sputter time. Based on the AES study mentioned earlier in this section, we estimated that the sputter rate is about 1.3 ML/min in this experiment. In Fig. 3 we can see that there is no noticeable decrease of the AES ratio during the initial sputter period. Therefore, the result of this experiment is in favor of the intermixing model.

3. Angle-resolved AES study

Angle-resolved AES (ARAES) is based on the strong forward scattering of Auger electrons with kinetic energies of a few hundred eV, by neighboring atoms.^{5,6} A direct result of the forward scattering is the enhancement of the AES intensity along the direction between the Auger-electron emitter and the scattering atom, resulting in a characteristic angular distribution of the AES intensity along certain directions. The forward scattering effect is significant typically only for the nearest- and next-nearest-neighbor distances, and so ARAES is an excellent technique to probe the local environment of a specific atom close to the surface. Figure 4 is a plot of ARAES spectra at several Fe coverages. The monitored peak is the Fe Auger transition at 706 eV excited by 5 keV

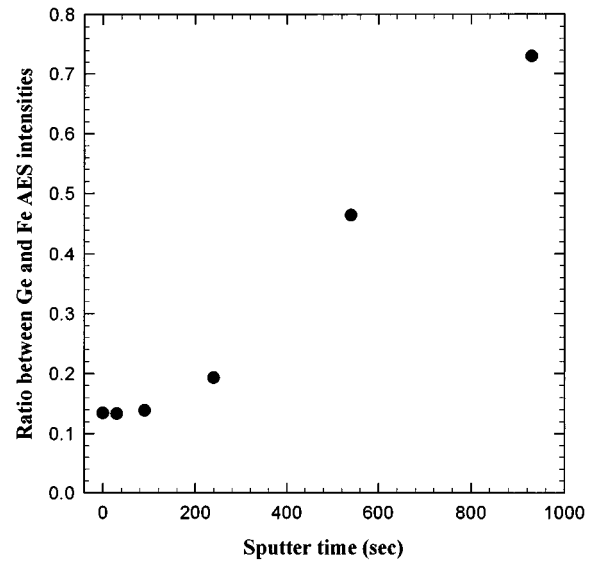


FIG. 3. Ratio between Ge and Fe AES intensities as a function of sputter time. The starting thickness of the Fe Film is 30 ML. The sputter rate calculated is about 1.3 ML/min.

primary electrons. The scans were taken as a function of the polar angle with the azimuthal angle fixed in the (010) plane. To present the data clearly, different vertical offsets have been added to the spectra except the 4 ML one. The data clearly demonstrate that the strong enhancement of the AES intensity at 0° and 45° , which is a signature of a cubic structure, only starts at 7 ML and is quickly saturated in 2–3 ML. This suggests that a cubic-type bonding arrangement between the iron atoms is only established at about 7 ML. Interestingly, this is the same coverage as that at which our

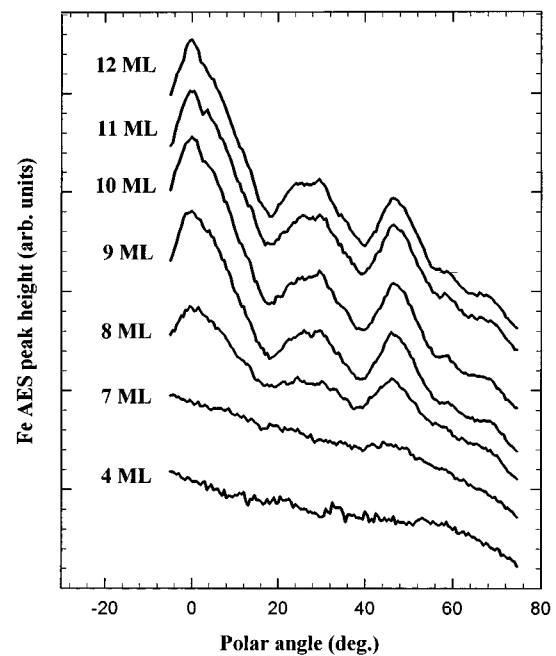


FIG. 4. Angle-resolved AES spectra of Fe films of various thicknesses. The monitored peak is the Fe Auger transition at 706 eV excited by a 5-keV electron beam. The scan is in the (010) plane.

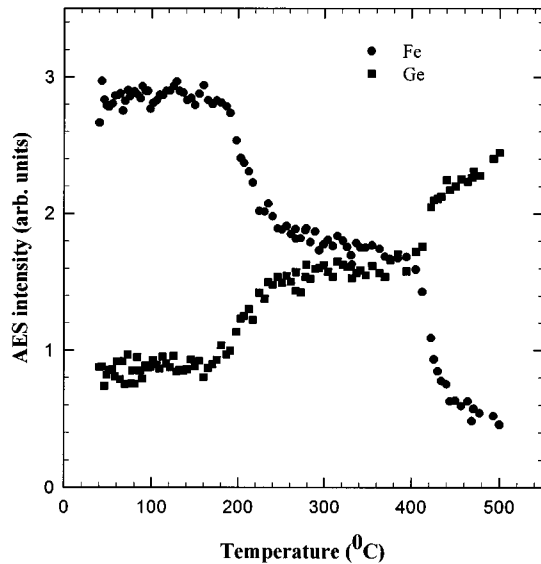


FIG. 5. Effect of annealing on a 12 ML Fe on Ge(100). The annealing temperature was ramped linearly at 2.4 °C per min.

LEED observations (Fig. 1), indicate that long-range order is also being established. Below 7 ML, the spectra are essentially featureless, although at higher sensitivity and better S/N , weak peaks around 0° and 45° for can be detected in films between 3 and 7 ML. Polar ARAES scans were also performed in the (011) azimuth to obtain more structural information about the overlayers. A similar Fe coverage dependence of the enhancement of the forward scattering peaks at 0 and 55° was observed, but no peak was observed at 35° . This clearly indicates that the Fe layer is growing in the bcc structure, since, for an fcc layer, a forward scattering peak should be observed at 35° along the (011) azimuth. This result is consistent with the LEED data.

B. Thermal stability

The thermal stability of a 12-ML Fe film was studied by monitoring the AES intensities as the temperature was ramped linearly from room temperature at 2.4 °C/min. Figure 5 plots the AES peak amplitudes of Fe and Ge as a function of annealing temperature. We can see that the peak amplitudes of Ge and Fe remain constant for temperatures $< 160^\circ\text{C}$. Between 240 and 400 °C, there is another plateau with the ratio of Fe AES amplitude to Ge AES amplitude close to 1. The Fe signal quickly disappears at temperatures above 400 °C. As discussed in Sec. III A, there is a small amount of Ge intermixed/segregated in/on the Fe film. No additional intermixing and/or segregation occurs between room temperature and 160 °C but significant intermixing clearly takes place above about 160 °C, which is probably the reason for the thick magnetic dead layer reported for 150 °C growth by Prinz.² It is likely that a surface alloy is formed between 160 and 400 °C. Based on the Auger sensitivity of Fe and Ge,⁷ the ratio of atomic concentrations of Ge and Fe in the intermixed region can be estimated as about 2:1. At 400 °C, the alloy apparently dissociated and Fe atoms quickly diffuse into the bulk of the Ge substrate.

Intermixing has always been a major concern in growing ultrathin ferromagnetic films on semiconducting substrates,

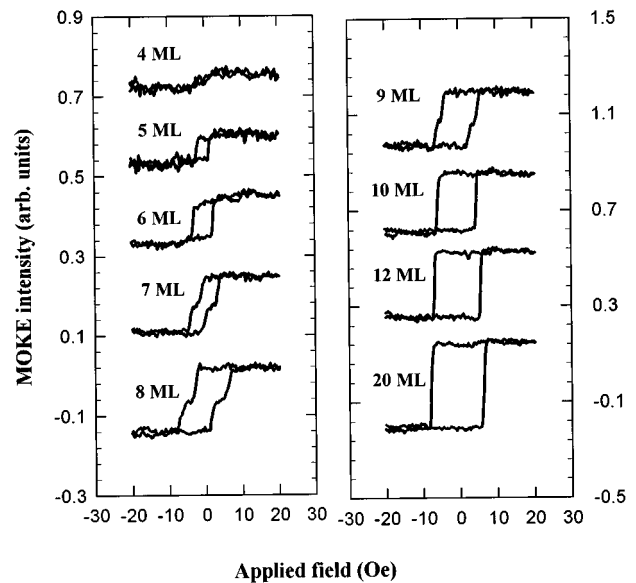


FIG. 6. Hysteresis loops measured with *in situ* MOKE for Fe films up to 20 ML. The MOKE system was set up in the longitudinal configuration and the applied field was along (010).

since it can create a thick magnetically dead layer. A well-known method used to prevent intermixing involves the growth of a buffer layer before deposition of the magnetic layer. For example, on the GaAs(100) surface, a thick Ag buffer layer is usually grown before deposition of the Fe film to avoid the intermixing. As we have seen so far, in the case of Fe on Ge(100), the intermixing is not severe for temperatures between 25 and 160 °C, and this will be true for lower temperatures. This is an important observation for the cases in which a buffer layer is not desirable.

C. Magnetic properties

Figure 6 plots the results of MOKE measurements of several Fe films with the applied field along the (010) direction. For Fe film thicknesses of less than 4 ML, no hysteresis loop was observed, and even at 4 ML there is only a trace of a hysteresis loop. A narrow loop appears at about 5–6 ML and then becomes a stepped loop between 7 and 9 ML. For Fe coverages greater than 10 ML and up to 20 ML, only single loops were observed. This transition from single to stepped to single loops was consistently observed in all experiments as a function of Fe coverage.

The first 3–4 ML of Fe is either magnetically dead or has an easy axis perpendicular to the film. This question cannot be resolved *in situ* with our MOKE system, which is set up in the longitudinal configuration. However, about the same thickness of dead layer was reported in the Fe/GaAs(100) case.⁸ The hysteresis loop first appears between about 4 and 6 ML and at these Fe coverages the structure of the films is still disordered (LEED), but some short-range bcc order has been established (ARAES).

In our FMR studies on the gold-capped Fe films grown on Ge(100) under conditions identical to those used for the films described in the present paper, we found that all the films studied (from 5 to 20 ML) have in-plane uniaxial anisotropy.⁸ As we have seen in the previous sections, the

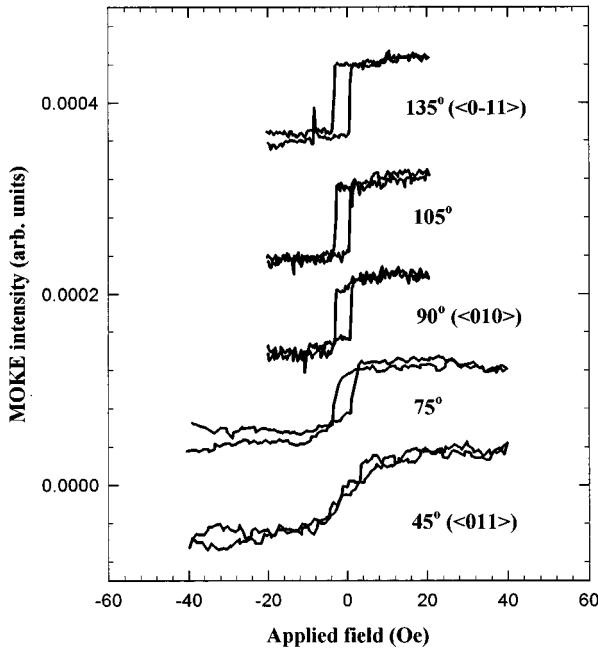


FIG. 7. Hysteresis loops measured with *ex situ* MOKE system on a gold-capped 6.5 ML Fe film grown on Ge(100) at room temperature. The angles indicated in the figure are the angles between the applied field and the $\langle 010 \rangle$ direction.

films have a bcc structure. Therefore, there must also be a cubic anisotropy energy contribution. The stepped loops between 7 and 10 ML are the result of the competition between the in-plane uniaxial and cubic anisotropies. For a very thin film, the uniaxial anisotropy may have a relatively large value. As the film becomes thicker, the film also becomes more bulklike and eventually the cubic anisotropy will dominate. Therefore, during the film growth process, the ratio of the cubic and uniaxial anisotropies varies, and this ratio should generally increase as the film thickness increases. As will be demonstrated below, this ratio (between the cubic anisotropy and the uniaxial anisotropy) determines the shape of the hysteresis loops.

Figure 7 shows hysteresis loops of a 6.5-ML Fe film capped with gold and measured with our *ex situ* MOKE system in the longitudinal configuration. The angles indicated in the figure are the angles between the applied field and the $\langle 010 \rangle$ direction in the sample plane. It is clear that the magnetic property lacks fourfold symmetry and that $\langle 011 \rangle$ and $\langle 0\bar{1}1 \rangle$ axes are not equivalent; the former behaves like a hard axis and the latter like a soft axis. Therefore, for this film we expect that the uniaxial anisotropy is relatively large and the uniaxial axis is along $\langle 0\bar{1}1 \rangle$. Similar results were also found for Fe on the GaAs(100) surface.¹⁰

In the following section, we describe the application of the coherent model¹¹ to model and interpret the hysteresis loops observed in Figs. 6 and 7. In doing so, we assume that the uniaxial axis is along $\langle 0\bar{1}1 \rangle$ for all film thicknesses. Therefore the energy density of the thin film can be written as

$$E = \frac{K_1}{4} \sin^2 2(\theta - \phi) + K_u \sin^2 \left(\frac{\pi}{4} + \theta - \phi \right) - HM \cos \theta, \quad (5)$$

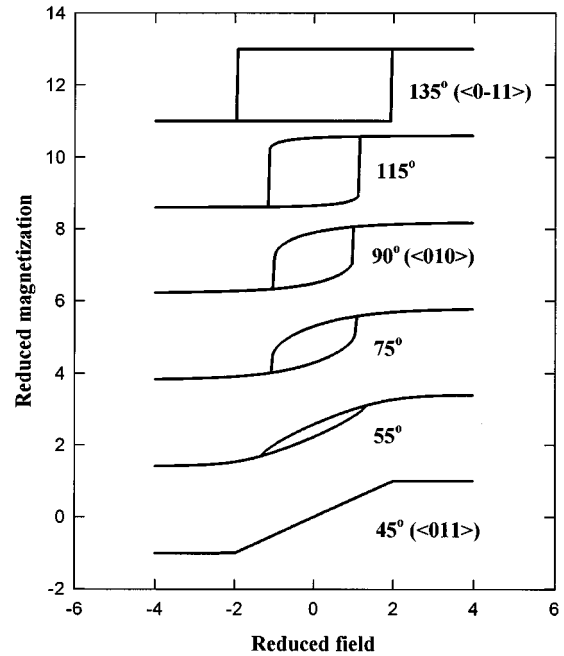


FIG. 8. Calculated hysteresis loops for a film with in-plane uniaxial anisotropy and with zero cubic anisotropy. The angles in the figure are the angles between the external field and the $\langle 010 \rangle$ direction.

where K_1 is the fourth-order crystalline cubic anisotropy, K_u is the in-plane uniaxial anisotropy, θ is the angle between \mathbf{M} and \mathbf{H} , and ϕ is the angle between \mathbf{M} and $\langle 010 \rangle$. In simulating the loops in Fig. 7, we let $K_1 = 0$, which corresponds to a film with uniaxial anisotropy and without cubic anisotropy. The results are presented in Fig. 8. In this figure, the reduced field is $(M/K_u)H$, and the reduced magnetization is really

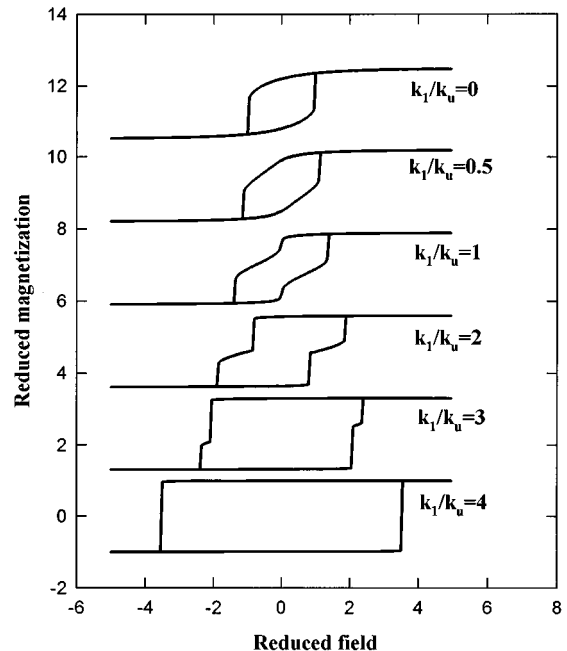


FIG. 9. Calculated hysteresis loops for films with different ratios of cubic anisotropy and in-plane uniaxial anisotropy. The external field is along $\langle 010 \rangle$.

$\cos(\theta)$. The angles indicated in the figure are the angles between the applied field and the $\langle 010 \rangle$ direction. The similarity between Figs. 7 and 8 shows that the uniaxial anisotropy is dominant for very thin Fe films on Ge(100). In simulating the results in Fig. 6, we let $\phi=0$, which corresponds to an applied field along $\langle 010 \rangle$. Figure 9 shows the results of the simulation. In this figure we see that with the applied field along $\langle 010 \rangle$, the stepped loops appear when the K_1 and K_u have comparable values. When K_1/K_u is very small or larger than about 4, a normal loop should be observed. It is interesting to note that the stepped loops appear at about the same Fe coverage as the LEED pattern reappears and approaches its maximum intensity and also at the same coverage at which the 45° peak in the ARAES spectra appears and grows (Secs. III A 1 and III A 3); this is precisely the region in which the bcc structure develops strongly. There is, therefore, a very good correlation between the structural and magnetic properties. Also, the result of the simulation is remarkably consistent with our FMR measurement,⁸ where we found that generally K_u decreases with Fe thickness while K_1 increase with Fe thickness, and K_1/K_u is about 0.5 at 5 ML, 1.8 at 8 ML, and 5.8 at 10 ML.

IV. CONCLUSIONS

We have studied the room-temperature growth of Fe on Ge(100) by LEED, AES, and ARAES, and the magnetic

properties by MOKE. The growth of Fe on Ge(100) initially occurs in a disordered fashion, clear evidence of formation of the cubic structure only appearing above 4 ML. Above 7 ML an ordered overlayer of bcc structure is formed. An AES study indicates that a small amount (about 6%) of Ge intermixes with the Fe film. The magnetic properties of the films are clearly dependent on the structure of the films. A narrow single loop was observed between 5 and 6 ML. The hysteresis loops become stepped over the next 3–4 ML (total coverages between 8 and 10 ML), becoming single loops again above 10 ML. Our calculation indicates that this single to stepped to single loop transition is the result of the increase of the ratio between the cubic anisotropy and the in-plane uniaxial anisotropy with the increase of the film thickness. Significant intermixing did not occur for temperatures below 160°C . Between 160 and 400°C a Ge-Fe alloy is formed with an atomic composition of 2 Ge to 1 Fe. With even higher annealing temperatures, Fe completely diffuses into the bulk Ge.

ACKNOWLEDGMENTS

The authors gratefully acknowledge helpful discussions with Bret Heinrich and Keith Griffiths, the technical assistance of Leighton Coatsworth, Dan O'Dacre, and Lawrence Green. NSERC is acknowledged for financial support.

¹E. Schloemann, R. Tustison, J. Weissman, and J. Van Hook, *J. Appl. Phys.* **63**, 3140 (1988).

²G. A. Prinz, in *Ultrathin Magnetic Structures II*, edited by B. Heinrich and J. A. C. Bland (Springer-Verlag, Berlin, 1994), p. 35.

³G. W. Anderson, P. Ma, and P. R. Norton, *J. Appl. Phys.* **79**, 5641 (1996).

⁴P. Ma, J. H. Horton, and P. R. Norton (unpublished).

⁵W. F. Egelhoff, *Solid State Mater. Sci.* **16**, 213 (1990).

⁶S. A. Chambers, *Surf. Sci. Rep.* **16**, 261 (1992).

⁷L. E. Davis, N. C. MacDonald, P. W. Palmberg, G. E. Raich, and R. E. Weber, *Handbook of Auger Electron Spectroscopy* (Physical Electronics Industries, Eden Prairie, Minnesota, 1976).

⁸P. Ma, P. R. Norton, and B. Heinrich (unpublished).

⁹M. Gester *et al.*, *J. Appl. Phys.* **80**, 347 (1996).

¹⁰J. J. Krebs, B. T. Jonker, and G. A. Prinz, *J. Appl. Phys.* **61**, 2596 (1987).

¹¹B. Dieny, J. P. Gavigan, and J. P. Rebouillat, *J. Phys.: Condens. Matter* **2**, 159 (1990).